Batch and continuous synthesis of well-defined Pt/Al_2O_3 catalysts for the dehydrogenation of homocyclic LOHCs

Yazan Mahayni[a,b], Lukas Maurer[a,b], Ina Baumeister[b], Franziska Auer[a] , Peter Wasserscheid[a,b]
Moritz Wolf[c,*]

[a] Forschungszentrum Jülich GmbH, Helmholtz-Institute Erlangen-Nürnberg for Renewable Energy (IEK-11), Erlangen, Germany

[b] Friedrich-Alexander-Universität Erlangen-Nürnberg (FAU), Lehrstuhl für Chemische Reaktionstechnik, Erlangen, Germany

[c] Karlsruhe Institute of Technology (KIT), Engler-Bunte-Institut & Institute of Catalysis Research and Technology, Karlsruhe, Germany

[*]Corresponding author. Address: Hermann-von-Helmholtz-Platz 1, 76344 Eggenstein-Leopoldshafen,, Germany. E-Mail-address: moritz.wolf@kit.edu

Abstract

In this work, the controlled synthesis of supported Pt nanoparticles with well-defined nanoparticle sizes from 1.9 to 6.0 nm and their application in the dehydrogenation of cyclic liquid organic hydrogen carrier (LOHC) molecules are demonstrated. For this purpose, a colloidal approach is used in which a stabilized Pt precursor solution is chemically reduced with aqueous solutions of sodium borohydride ($NaBH_4$). In this batch process, an increased pH increases the stability of the reduction solution and thus enhances the control of the size of the resulting Pt nanoparticles. Various synthesis parameters are varied and their effects on the properties of the Pt nanoparticles are studied. Additionally, the nanoparticles were supported on powder Al_2O_3 support and the general suitability of the catalysts for the dehydrogenation of the LOHC perhydro benzyltoluene (H12-BT) is demonstrated. The transferability of the catalyst synthesis route from powder to shaped supports, as commonly used in LOHC dehydrogenation reactors, is successfully demonstrated. Moreover, a successful upscaling of the synthesis procedure is realized, where larger amounts of catalysts are synthesized without significant deviations in nanoparticle size and catalytic activity. Finally, a continuous synthesis of Pt/Al_2O_3 catalysts is implemented using a microfluidic reactor. The prepared catalysts from small-scale, large-scale, and continuous syntheses display a comparable Pt-based productivity in the dehydrogenation of H12-BT.

Introduction

Numerous studies identified the importance of platinum nanoparticle morphology in a wide variety of heterogeneously catalyzed reactions.[1-6] This also includes the dehydrogenation of cyclic liquid organic hydrogen carriers (LOHCs) over Pt/Al_2O_3 catalysts. For instance, the group of Somorjai intensively studied the structure sensitive behavior of the dehydrogenation of cyclohexane[7-8] and methylcyclohexane (MCH).[9] For the dehydrogenation of the LOHC perhydro dibenzyltoluene (H18-DBT), remarkable activity changes were observed by Auer *et al.* for a nanoparticle size range from 1.2 to 4.6 nm. Specific initial productivities of the corresponding catalysts in the dehydrogenation of H18-DBT at 310 °C in the range of 2 to 4 $g_{H2}\ g_{Pt}^{-1}\ min^{-1}$ were reported.[2] This emphasizes the need for scalable synthesis routes for Pt/Al_2O_3 catalysts that allow precise control of the size of the platinum nanoparticles.

Pt/Al_2O_3 catalysts are commonly synthesized via wet impregnation of the support with an aqueous Pt precursor solution.[10-12] This route offers several advantages, such as high dispersion of the metal particles and simple scalability. However, required thermal treatment during subsequent processing of the catalysts i.e., calcination in air at temperatures between 300 and 500 °C[13] or reduction under hydrogen atmosphere at 200 to 600 °C,[14] is associated with challenges. At such elevated temperatures, enhanced particle mobility may result in sintering, which has been observed for thermal treatments under both oxidative[15-18] and H_2-containing[19-20] environment. These effects may alter the morphology of the Pt nanoparticles and hence the specific catalytic activity in structure sensitive dehydrogenation reactions. Contrary, direct chemical reduction to metallic Pt can circumvent thermal treatment prior to catalytic application. For example, sodium borohydride ($NaBH_4$) has been widely employed as a reducing agent for the colloidal synthesis of transition metals.[21-29] Moreover, chemical reduction has proven to yield well-defined Pt nanoparticles with distinct control over particle size in combination with a narrow particle size distribution.[21-24] This is due to the adjustable amount of the liquid reducing agent and thus the strength and speed of the reduction compared to alternative methods e.g., with gaseous H_2. In addition, the utilization of steric capping agents, such as polyvinylpyrrolidone (PVP), is essential to circumvent agglomeration of the synthesized nanoparticles.[30-31] For catalytic applications, the separately synthesized, chemically reduced nanoparticles can be immobilized onto a support.

In this work, we study the influence of the synthesis parameters on the size of nanoparticles in Pt/Al_2O_3 catalysts obtained via the colloidal synthesis with chemical reduction and immobilization

on the support. Aside from catalytic testing in the dehydrogenation of H18-DBT, the transferability of the synthesis route from powder to shaped Al_2O_3 supports is studied as the latter are required for state-of-the-art commercial LOHC dehydrogenation reactors.[32-33] To overcome mass transfer limitations, egg-shell catalysts are used in the dehydrogenation of homocyclic LOHCs, such as perhydro dibenzyltoluene[34-35] and perhydro benzyltoluene.[36-37] Lastly, we describe the scale-up of the colloidal synthesis to a fivefold batch size to produce 50 g of shaped Pt/Al_2O_3 egg-shell catalysts with well-defined nanoparticle size. Additionally, the synthesis process is transferred from batch to continuous operation to enable large-scale catalyst production in the absence of thermal processing.

Methodology

Catalyst synthesis

The supported Pt nanoparticle catalysts were synthesized by modifying procedures described in literature.[22, 38] At first, the capping agent polyvinylpyrrolidone (PVP, MW 40 000, Sigma Aldrich) was dissolved in 50 mL of Millipore water and ultra-sonicated for 15 min. An amount of 52 mg of chloroplatinic acid (H_2PtCl_6, Sigma Aldrich) was added to the PVP solution followed by ultra-sonication for 1 min. The obtained solution was magnetically stirred at 1500 rpm before rapid injection of the reducing agent. Chemical reduction was induced through the addition of an aqueous solution of sodium borohydride ($NaBH_4$, 33mM in Millipore Water, Acros Organics), which was cooled in an ice bath to limit decomposition of $NaBH_4$ via hydrolysis.[39-41] Different volumes of $NaBH_4$ solution were added (0.2-2.4 mL) to yield various sizes of the Pt nanoparticles. After 1 min of stirring, the nanoparticles were immobilized onto an Al_2O_3 powder (PURALOX TH100/150, Sasol Germany) or on shaped Al_2O_3 tablets (hollow cylinders 5 x 5 x 2.2 mm (L x D_{out} x D_{in}), Sasol Germany) and left overnight under moderate stirring to ensure homogeneous distribution of the nanoparticles on the support. A loading of 0.2 wt% Pt was targeted for all catalysts by the addition of the appropriate amount of alumina support (typically 10 g). Finally, the solvent was evaporated at 80 °C and 250 mbar in a rotary evaporator to obtain the catalyst for analysis and catalytic testing without further treatment. Modified procedures deviating from this standardized method are described in the manuscript where applicable.

Material characterization

N_2 physisorption was applied in a Tristar II Plus (Micromeritics) for the evaluation of the textural properties of the support materials e.g., surface area, pore size, and pore volume. The samples were degassed at 250 °C and ~0.01 mbar under a flow of He, while the specific surface area was determined via the BET method in the relative pressure range 0.05-0.35 and the BLH method was applied to obtain pore characteristics.

Pt loadings of the catalysts were analyzed by means of inductively coupled plasma optical emission spectroscopy (ICP-OES) using a Ciros CCD device (Spectro Analytical Instruments GmbH). The solid samples were dissolved in a concentrated HCl:HNO_3:HF mixture with a 3:1:1 volumetric ratio and microwave digestion. The instrument was calibrated with standard solutions of Pt prior to the measurements.

High-resolution transmission electron microscopy (HR-TEM) was conducted for size analysis of the supported Pt nanoparticles in a CM30 (Philips). For sample preparation, small amounts of the Pt/Al_2O_3 catalysts were dispersed in ethanol and drop-casted on 300 mesh copper grids with lacey carbon coating (Plano GmbH). The size of 150-400 Pt nanoparticles from different areas of the sample were analyzed individually by two operators using ImageJ to obtain size distributions.[42]

CO pulse chemisorption was used to probe the accessible active sites of the supported nanoparticles. For this, 300 mg of the respective Pt/Al_2O_3 catalyst materials were analyzed in an Autochem II 2920 (Micromeritics). The samples were flushed by a continuous flow of 20 mL min^{-1} He with intermittent dosing of 368 µL CO to quantify the amount of adsorbed CO.

Dehydrogenation of H12-BT

All dehydrogenation experiments in this work were conducted in a 100 mL three-neck round-bottom flask. H12-BT (degree of hydrogenation > 97.5%; Hydrogenious LOHC Technologies GmbH) was weighed into the flask at room temperature. Hereafter, a thermocouple, a catalyst dosing device and an Ar inlet line were connected through the side necks, while an intensive condenser was attached to the middle-neck. The corresponding amount of catalyst material to realize a Pt:H12-BT ratio of 0.1 mol% was loaded into the dosing device. Before the start of the experiments, an Ar flow of 300 mL min^{-1} was set by a mass-flow controller (Bronkhorst Deutschland Nord GmbH). The system was then heated to the desired reaction temperature of

250 °C by a heating jacket with a temperature controller. The catalyst was released into the pre-heated liquid phase upon stabilization of the temperature to initiate the reaction. To quantify the amount of released H_2, a thermal conductivity detector (Messkonzept GmbH) was used to analyze the concentration of H_2 in the off gas at an internal set temperature of 60 °C. From the volumetric flow ratio $X_{H_2/Ar}$, the applied argon flow rate $\dot{V}_{Ar}$, the density of hydrogen ρ_{H_2} at 60 °C, the catalyst mass $m_{catalyst}$ and the Pt loading of the catalyst w_{Pt}, the temporally resolved productivity can be calculated as follows:

$$Productivity\ (t) = \frac{X_{\frac{H_2}{Ar}}(t) \cdot \dot{V}_{Ar} \cdot \rho_{H_2}}{m_{catalyst} \cdot w_{Pt}} \qquad (1)$$

In addition, the degree of dehydrogenation (DoDH) can be derived with the know amount of maximum reversibly bound H_2 in H12-BT $n_{H2,max}$:

$$n_{H_2}(t) = \int_0^t X_{\frac{H_2}{Ar}} \cdot \dot{V}_{Ar} \cdot \frac{\rho_{H_2}}{M_{H_2}}\, dt \qquad (2)$$

$$DoDH = \frac{n_{H_2}(t)}{n_{H_2,max}} \qquad (3)$$

Results and discussion

Based on previous works by Auer *et al.*[2], the selected Al_2O_3 powder support provides suitable properties for the dehydrogenation of homocyclic LOHC compounds e.g., H18-DBT or H12-BT. A specific surface area of 162 $m^2\ g^{-1}$ and a mean pore diameter of 20 nm were determined by means of N_2 physisorption (Table 1). A sufficiently large specific surface area allows for a good dispersion of the platinum nanoparticles on the support with large inter-particle distances, whereas a large mean pore diameter minimizes mass transport limitations due to the bulky LOHC molecules.[18]

Table 1: Morphology of powder and shaped Al_2O_3 supports.

Support	Surface area / $m^2\ g^{-1}$	Mean pore diameter / nm	Particle size
Powder[a]	162	20	35 µm (d_{50})
Shaped[43]	180	n.a.	5 x 5 x 2.2 mm (LxBxH)

[a] As determined by means of N_2 physisorption

For a first conceptual test, a Pt/Al_2O_3 catalyst was prepared. First, colloidal Pt nanoparticles were synthesized using a PVP:Pt ratio of 10:1 and a $NaBH_4$:Pt ratio of 0.31 mol_{NaBH4} mol_{Pt}^{-1} based on ratios in literature.[22, 34, 38] A 0.20 wt.% Pt/Al_2O_3 catalyst was targeted by immediate immobilization of the nanoparticles onto the powder Al_2O_3 support. An actual Pt loading of 0.18 wt.% was determined by means of ICP-OES. Size analysis by high-resolution transmission electron microscopy (HR-TEM) suggests a mean diameter of 2.1 nm (Figure 1a). The catalyst was then tested in the dehydrogenation of H12-BT at 250 °C to assess the general suitability of chemical reduction during colloidal synthesis for subsequent catalytic applications. The observed initial productivity of the synthesized Pt/Al_2O_3 catalyst of up to 0.5 g_{H2} g_{Pt}^{-1} min^{-1} (Figure 1b) during batch dehydrogenation is comparable with reported values of 0.7 to 0.9 g_{H2} g_{Pt}^{-1} min^{-1} by Rüde *et al.*[37], who tested a commercial, selectively poisoned catalyst at significantly higher temperature of 290 °C. Hence, the catalysts synthesized via immobilization of colloidal chemically reduced nanoparticles is generally catalytically active and can be applied without any pre-treatment.

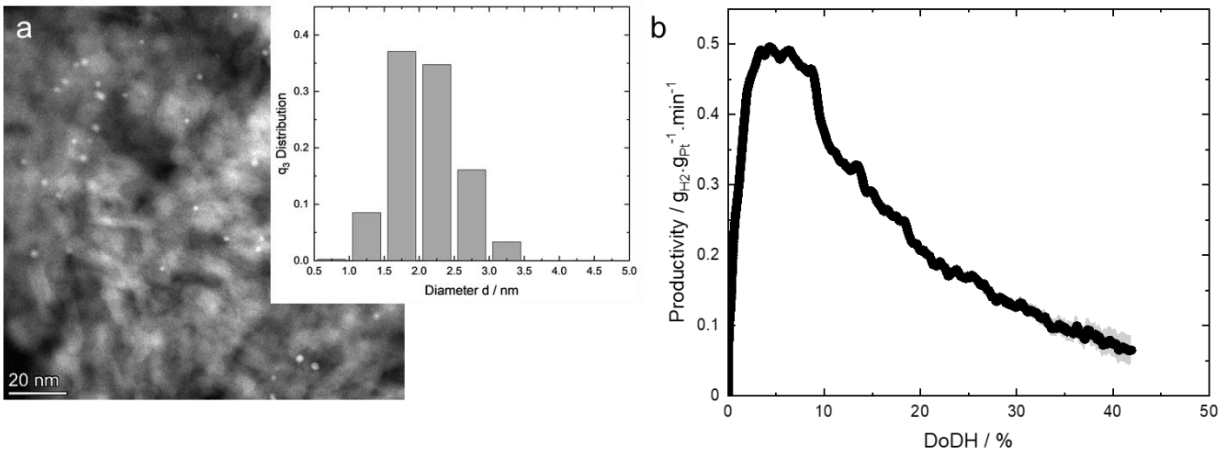

Figure 1: (a) HR-TEM micrograph and particle size distribution of colloidal, chemically reduced Pt nanoparticles immobilized onto a powder Al_2O_3 support with obtained size distribution and (b) productivity as a function of degree of dehydrogenation (DoDH) of H12-BT during semi-batch dehydrogenation. Reaction conditions: T = 250 °C, Pt:LOHC = 1:1000 mol_{Pt} mol_{LOHC}^{-1}, F_{Ar} = 300 mL min^{-1}, $t_{Reaction}$ = 120 min, catalyst loading = 0.2 wt.% Pt. Synthesis conditions: Batch procedure with powder Al_2O_3 support, PVP:Pt = 10 g_{PVP} g_{Pt}^{-1}, $NaBH_4$:Pt = 0.31 mol_{NaBH4} mol_{Pt}^{-1}.

Pt nanoparticle size control in batch procedure

First, the influence of the gravimetric ratio of PVP:Pt on the nanoparticle size in the respective catalysts was evaluated. However, no significant change in the resulting Pt nanoparticle size of 2.2 nm was observed in the range of 5:1 to 15:1 (Figure 2). Only the highest ratio of 20:1 resulted in larger nanoparticles, but the synthesis was less reproducible, most likely due to an insufficiently

controlled particle growth. Since the large PVP molecules (40,000 g mol^{-1}) may prevent access to the Pt surface, the accessibility of the metallic Pt sites for different PVP:Pt ratios was probed by means of CO pulse chemisorption (Figure 2). A detrimental influence of surfactants on catalysis has previously been reported,[44-45] which renders synthesis routes with low to zero amount of surfactants highly desirable.[46] Low PVP:Pt ratios result in a specific adsorption of CO of approx. 10 µmol g^{-1}, which is close to the expected amount for completely accessible spherical 2.2 nm nanoparticles (13.3 µmol g^{-1}). Interestingly, the amount of adsorbed CO decreases below 4 µmol g^{-1} when increasing the PVP:Pt ratio to 15 g_{PVP} g_{Pt}^{-1}. This indicates blockage of Pt surface by the bulky stabilizer at PVP:Pt ratios ≥15. As the CO adsorption capacity is comparable for the lower ratios of 5 and 10 g_{PVP} g_{Pt}^{-1}, no significant hindrance is expected for these low PVP:Pt ratios and 5 g_{PVP} g_{Pt}^{-1} was selected for subsequent catalysts syntheses.

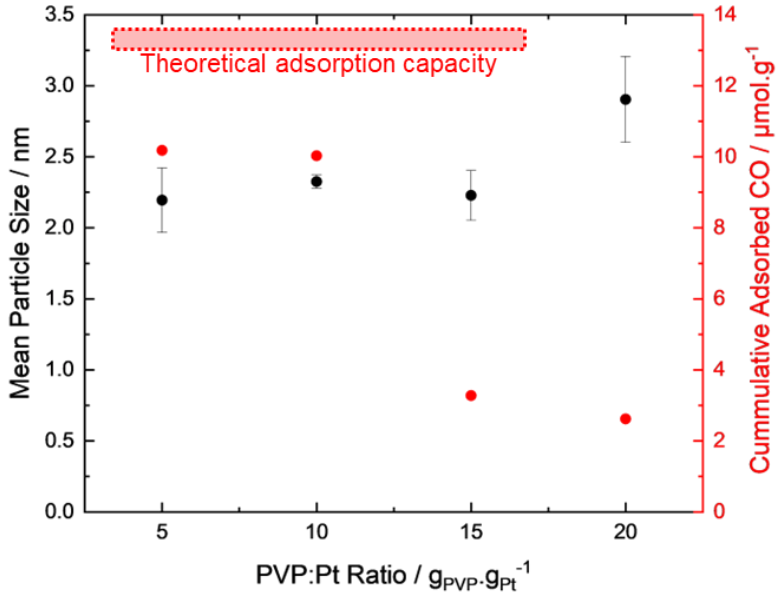

Figure 2: Influence of the specific amount of capping agent PVP on the size of synthesized Pt nanoparticles and the cumulative amount of adsorbed CO. Red box indicates the approximated CO adsorption capacity for the smaller nanoparticle sizes for full accessibility of the Pt surface. Synthesis conditions: Batch procedure with $NaBH_4$:Pt ratio = 0.31 mol_{NaBH4}·mol_{Pt}^{-1}. Error bars represent the standard deviation of mean nanoparticle size from three reproductions.

Analogous to the previous experiments with varying amounts of capping agent, the influence of the amount of reducing agent was also studied. Since the potential extent of metal reduction is linked to the utilized amounts of both, reducing agent and metal precursor, the molar $NaBH_4$:Pt ratio is herewith considered. This ratio is systematically varied in the range of 0.21 to 0.47 mol_{NaBH4} mol_{Pt}^{-1}. Expectedly and in agreement with the model of particle formation proposed by LaMer *et*

al.[35-36], the obtained platinum particle size is strongly dependent on the amount of $NaBH_4$ used for the reduction (Figure 3). Increased $NaBH_4$:Pt ratios result in a higher monomer concentration and, consequently, a faster nucleation rate. Hence, the monomer concentration remains beyond the critical supersaturation for longer durations, enriching the particle nucleation regime. Nevertheless, if the $NaBH_4$:Pt ratio is further increased, the size of randomly formed clusters increases due to the prompt monomer formation. This induces the formation of larger nuclei that contribute to a rapid drop in monomer concentration below the critical supersaturation i.e., terminating the nucleation regime and initiating particle growth.[47] Moreover, rapid reduction at the highest $NaBH_4$:Pt ratio may cause the formation of inhomogeneities within the suspension, which leads to a broadening of the particle size distribution and lower reproducibility. A similar behavior regarding the correlation between the applied $NaBH_4$:Pt ratio and the resulting size of PVP protected nanoparticles is described by Bedia et al.[48] Overall, an increase of the $NaBH_4$:Pt ratio leads to an increase in the nanoparticle size covering a size range of 2 to 6 nm. All $NaBH_4$ solutions were diluted, which generally facilitates the synthesis of small well-defined nanoparticles with narrow size distributions. This is again in agreement with LaMer *et al.*[49] The average particle size of the prepared and immobilized nanoparticles was analyzed by HR-TEM. Two exemplary micrographs and the corresponding narrow particle size distributions of catalysts synthesized with $NaBH_4$:Pt ratios of 0.21 and 0.47 $mol_{NaBH4}\ mol_{Pt}^{-1}$ are shown in Figure 4.

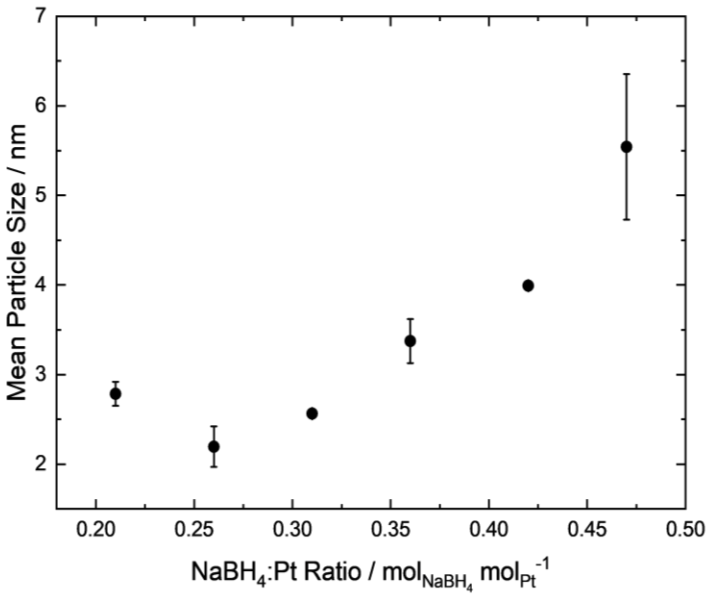

Figure 3: Influence of the specific amount of aqueous reducing agent $NaBH_4$ on the size of synthesized platinum nanoparticles. Synthesis conditions: Batch procedure with PVP:Pt ratio = 5 $g_{PVP}\ g_{Pt}^{-1}$. Error bars represent the standard deviation of the average value over three reproductions.

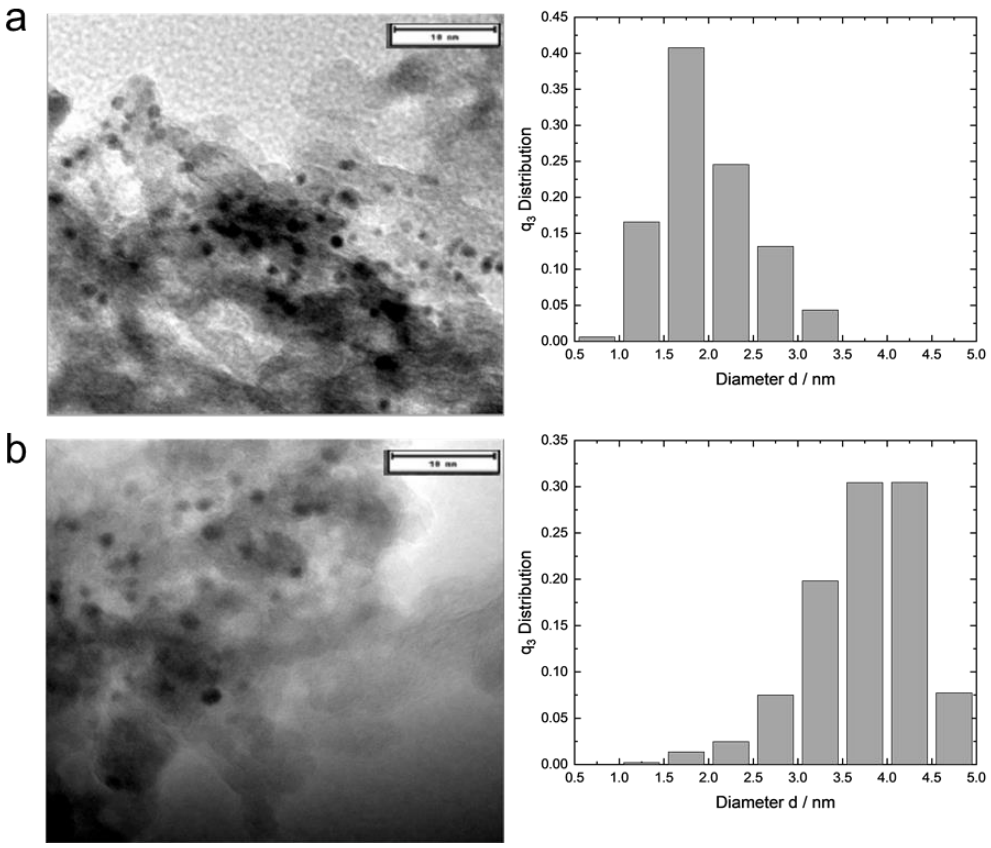

Figure 4: HR-TEM bright-field micrographs (scale bars: 10 nm) and Pt nanoparticle size distributions for Pt/Al_2O_3 catalysts synthesized with NaBH4:Pt ratios of (a) 0.26 and (b) 0.47 mol_{NaBH4} mol_{Pt}^{-1} resulting in mean platinum particle sizes of 2.0 and 4.7 nm, respectively. Synthesis conditions: Batch procedure with PVP:Pt ratio = 5 g_{PVP} g_{Pt}^{-1}.

The lowest $NaBH_4$:Pt ratio resulted in an opposite trend, leading to the formation of slightly enlarged nanoparticles. This may be due to the weak reduction force of the diluted reducing agent, which results in a slow formation of metal monomers *i.e.*, metallic Pt. Accordingly, the nucleation rate is similarly slow. This is due to the consumption of the slowly formed Pt monomers during the nucleation phase, which results in a quick drop in monomer concentration shortly after the critical supersaturation is exceeded. During the following growth regime, the ongoing reduction of platinum mostly contributes to particle growth rather than to the formation of new nuclei.

For the following catalyst syntheses, a $NaBH_4$:Pt ratio of 0.31 mol_{NaBH4} mol_{Pt}^{-1} was selected as the obtained particle size is sufficiently small to enable high Pt dispersions and the particularly high reproducibility.

Immobilization of Pt nanoparticles onto shaped supports

Commonly, Pt/Al_2O_3 shaped catalysts for the dehydrogenation of H18-DBT and H12-BT are synthesized via wet impregnation.[34-35] Strong interaction via electrostatic adsorption enables high dispersions and allows for the desired egg-shell distribution of the active component and also determine the nanoparticle size or even shape.[10, 50] Herein, the separate synthesis with subsequent immobilization of nanoparticles on a support material enables the preservation of their well-defined structure, while an appropriate distribution of the well-defined nanoparticles on the support material may be challenging. To accommodate immobilization onto shaped supports, the drying procedure in a rotary evaporator was divided into two sections: slow nanoparticle deposition at a moderate pressure of 250 mbar, followed by solvent evaporation at 35 mbar combined with a faster rotation of the synthesis flask (150 vs. 50 rpm). This procedure facilitated the penetration of the outer layers of the shaped support by dispersed nanoparticles, which already contain immobilized Pt nanoparticles. The homogeneity of the obtained shaped catalyst was thereby significantly improved (Figure 5).

Figure 5: Photograph of four batches of synthesized Pt/Al_2O_3 with optimized immobilization onto hollow cylinders. Synthesis conditions: Batch procedure, PVP:Pt ratio = 5 g_{PVP} g_{Pt}^{-1} and $NaBH_4$:Pt ratio = 0.31 mol_{NaBH4} mol_{Pt}^{-1}.

To evaluate the performance of the shaped catalysts in the dehydrogenation of H12-BT, Pt nanoparticles with an average diameter of 2.3 nm were synthesized and immobilized onto Al_2O_3 support material, both in powder and shaped form. The catalytic testing was performed in a semi-batch dehydrogenation experiment at 250 °C (Figure 6). The initial productivity of the shaped catalysts was slightly reduced, while H_2 release at higher DoDH was facilitated resulting in

comparable DoDHs of 42% and 46% after 120 min for the powder and shaped catalysts, respectively, after two hours reaction time. The initial divergence may be caused by mass transport limitations in case of the shaped catalyst, as large amounts of gaseous H_2 are released during this initial phase of the semi-batch dehydrogenation. However, this effect is not very pronounced due to the low egg-shell thickness. Peters et al.[51] studied the macrokinetic effects in perhydro-N-ethylcarbazole (H12-NEC) dehydrogenation by using egg-shell catalysts with various shell thicknesses. Based on their findings for H12-NEC, the absence of mass transport limitations for a reaction at 250 °C with a catalyst of approximately 5 µm shell thickness can be assumed.

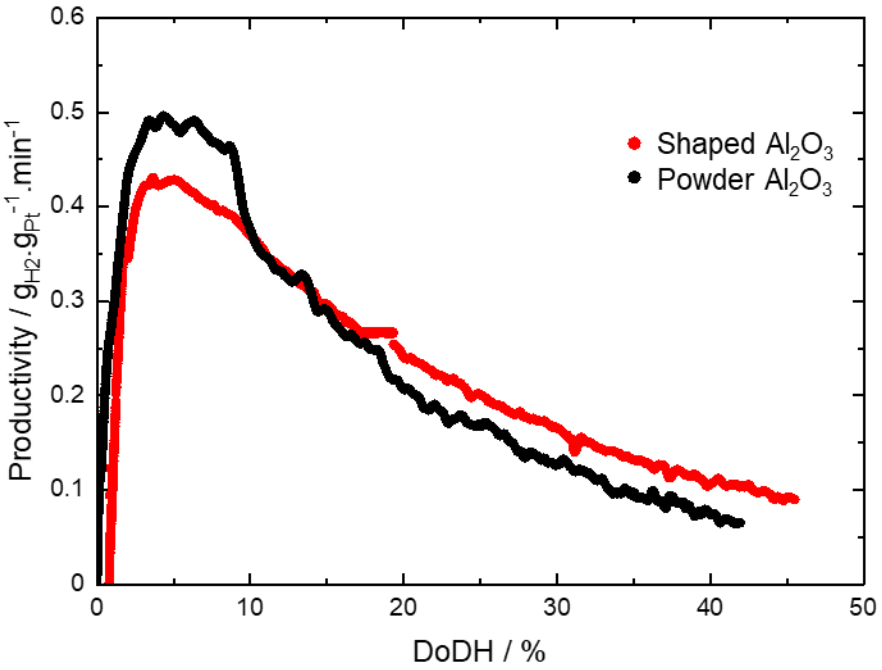

Figure 6: Productivity of Pt as a function of the degree of dehydrogenation (DoDH) for synthesized Pt/Al_2O_3 powder and shaped catalysts with Pt nanoparticle sizes of 2.3 nm during semi-batch dehydrogenation of H12-BT. Reaction conditions: T = 250 °C, $m_{Catalyst}$= 10 g, Pt: LOHC = 1:1000 mol_{Pt} mol_{LOHC}^{-1}, F_{Ar} = 300 mL·min^{-1}, $t_{Reaction}$ = 120 min, catalyst loading = 0.2 wt.%. Synthesis conditions: Batch procedure with PVP:Pt ratio = 5 g_{PVP} g_{Pt}^{-1}, $NaBH_4$:Pt ratio = 0.31 mol_{NaBH4} mol_{Pt}^{-1}.

To further investigate the scalability of the presented colloid chemical approach, a fivefold scale-up of the batch synthesis of well-defined platinum nanoparticles with a mean particle size of 2.3 nm with subsequent immobilization on shaped alumina yielding 50 g of Pt/Al_2O_3 catalysts was conducted. The performance during dehydrogenation of H12-BT at 250 °C is even improved (Figure 7) when compared to the catalyst synthesized on a small scale with a total amount of 10 g.

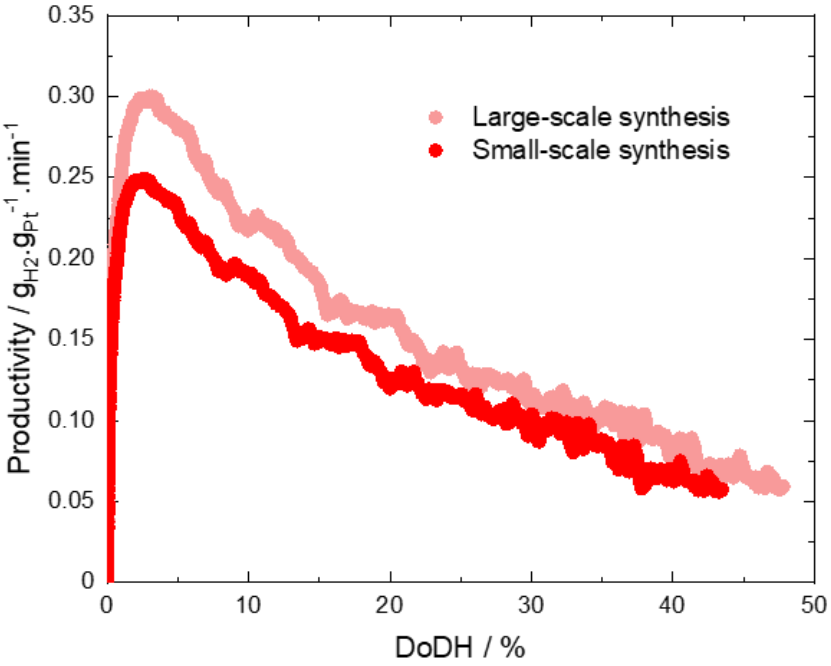

Figure 7: Productivity of Pt as a function of the degree of dehydrogenation (DoDH) of H12-BT during semi-batch testing of the fivefold Pt/Al_2O_3 shaped catalyst compared to the small-scale synthesis. Reaction conditions: T = 250 °C, Pt:LOHC = 0.0001 mol_{Pt} mol_{LOHC}^{-1}, F_{Ar} = 300 mL·min^{-1}, $t_{Reaction}$ = 120 min, catalyst loading = 0.2 wt.% m_{Pt}^{-2}. Synthesis conditions: Batch procedure with PVP:Pt ratio = 5 g_{PVP} g_{Pt}^{-1}, $NaBH_4$:Pt ratio = 0.31 mol_{NaBH4} mol_{Pt}^{-1}.

Continuous Synthesis

With regard to a further upscaling of the synthesis of well-defined Pt nanoparticles, especially with respect to the production of larger catalyst quantities for use in technical reactors, a continuous nanoparticle synthesis is of special interest. Here, the long-term stability of the reducing agent is of great importance as it is not consumed immediately. In literature, stabilization of the reducing agent $NaBH_4$ by NaOH has been ascribed to the pH dependency of its hydrolysis. A larger pH value preserves its reducing ability, and thus affects particle formation. Usually, a pH of 12 is targeted as the half-life of the reducing agent increases from 9.1 min (aqueous solution at pH 9) to 6.3 days (pH 12).[52-55] The role of pH adjustment during the synthesis of nanoparticles with narrow size distributions over an extended particle size range was examined first. Various amounts of $NaBH_4$ were dissolved in 10 mM NaOH solution (pH 12) and used for the synthesis of Pt nanoparticles. The modification of the batch synthesis with stabilized reducing agent resulted in a particle size range of 1.8 to 2.8 nm (Figure 8), which is smaller than without the use of NaOH. However, the control of the final particle size increases drastically.

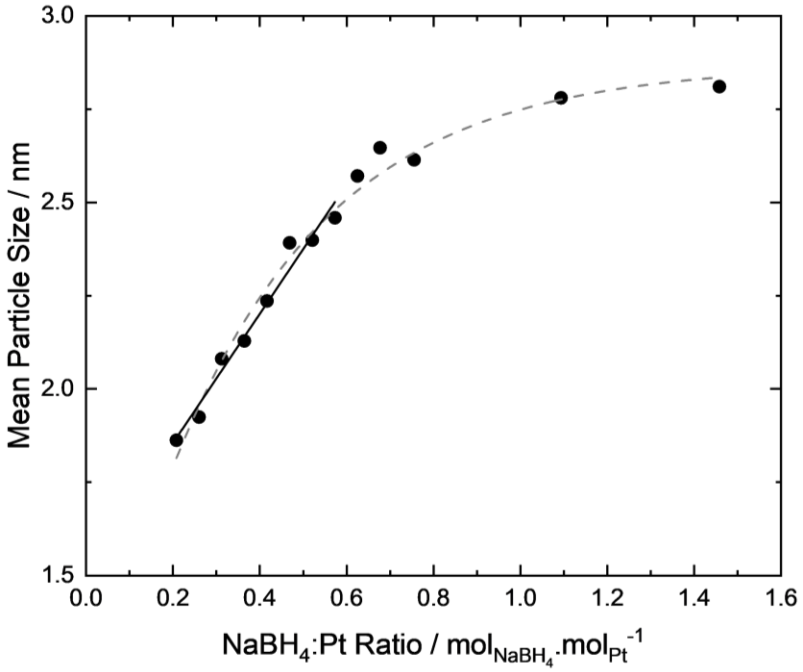

Figure 8: Influence of the specific amount of basic reducing agent $NaBH_4$ on the size of Pt nanoparticles. Synthesis conditions: Batch procedure with powders, PVP:Pt ratio = 5 g_{PVP} g_{Pt}^{-1}, c_{NaOH} = 10 mM. Dashed line represents exponential fit of the whole range. Solid line represents linear fit according to Equation (4).

For $NaBH_4$:Pt ratios exceeding 0.7 mol_{NaBH4} mol_{Pt}^{-1}, the obtained Pt nanoparticle sizes increase only marginally with increasing $NaBH_4$:Pt ratio and strive towards a plateau of a maximum nanoparticle size of 2.8 nm. This threshold was also observed by Van Rheenen *et al.*[53] with an even higher $NaBH_4$:Pt ratio of 18.3 mol_{NaBH4} mol_{Pt}^{-1}, suggesting 2.8 nm as the maximum achievable particle size in the applied colloidal synthesis with basic $NaBH_4$ solutions at pH 12 under ambient conditions. Within the range of 0.2 to 0.7 mol_{NaBH4} mol_{Pt}^{-1}, the mean Pt nanoparticle sizes exhibit a linear dependency with respect to the $NaBH_4$:Pt ratio. These findings emphasize the importance of a consistent and controllable reduction force for a highly size-selective synthesis of Pt nanoparticles. The linear correlation in the mentioned range (0.2-0.7 mol_{NaBH4} mol_{Pt}^{-1}) may be described by Equation (4):

$$d_v = \left(1.73 \cdot \left(\frac{n_{\mathrm{NaBH_4}}}{n_{\mathrm{Pt}}}\right) + 1.51\right) \mathrm{nm} \qquad (4)$$

With the successful stabilization of the reducing agent, a continuous synthesis of well-defined Pt nanoparticles can be implemented. Therefore, a microfluidic reactor (R-01) in combination with a two-channel syringe pump (P-01) was used. The two stock solutions (aqueous Pt-PVP and NaOH

stabilized $NaBH_4$ solutions) were provided in separate syringes (B-01 and B-02) and the resulting nanoparticle solution is collected in a round bottom flask (B-03). The microfluidic setup (Figure 9) is comparable to syntheses applied in literature.[56-58] Three syringe combinations were investigated (Table 2).

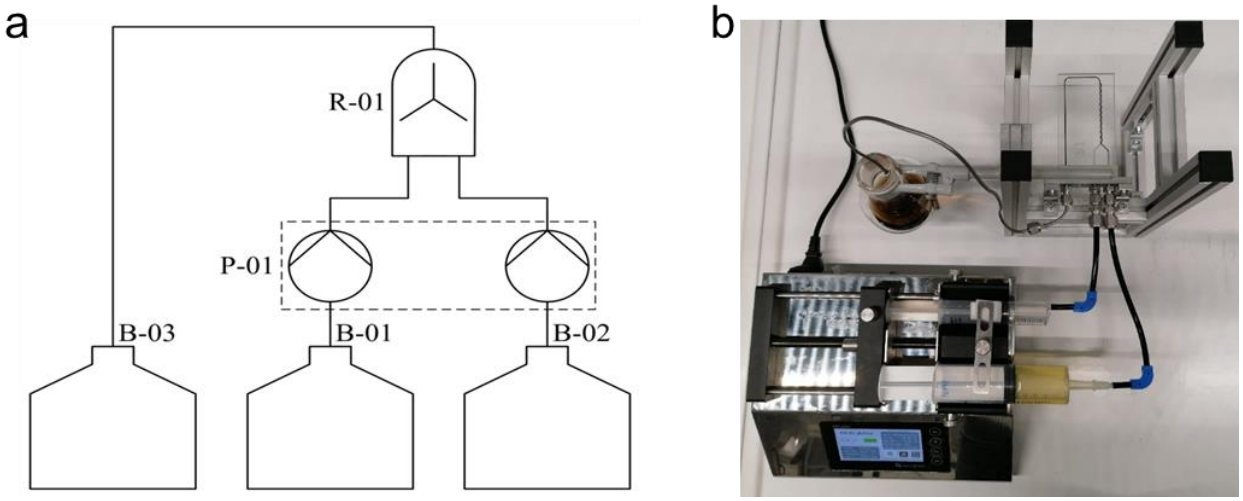

Figure 9: (a) Schematic illustration and (b) photograph of the laboratory setup for the continuous microfluidic synthesis of Pt nanoparticles.

Table 2: Investigated syringe combinations for the continuous synthesis of Pt nanoparticles. Large syringe: Pt-PVP solution; small syringe: NaOH stabilized $NaBH_4$ solution.

Combination	$V_{large\ syringe}$ [mL]	Length [cm]	$V_{small\ syringe}$ [mL]	Length [cm]	Flow rate ratio* [-]
A	30	11	20	9	1.54
B	30	11	10	7.5	3.57
C	100	13.5	30	9	6.50

* Flow rate ratio = (syringe diameter ratio)^2

Continuous nanoparticle syntheses were performed with the combinations A, B and C and the obtained nanoparticle sizes were analyzed. Based on the findings from previous batch syntheses, the respective stock solutions were prepared with the PVP:Pt and $NaBH_4$:Pt ratios required to target platinum nanoparticles with a particle size of 2.4 nm (5 g_{PVP} g_{Pt}^{-1}, 0.47 mol_{NaBH4} mol_{Pt}^{-1}, 10 mM NaOH). According to literature, a flow rate of 0.84 mL min^{-1} was set for the Pt-PVP solution in the large syringe.[59] The platinum nanoparticles from the continuous syntheses with the different syringe combinations exhibit mean particle diameters of 2.66 (A), 2.69 (B) and 2.68 nm

(C) according to analysis by means of HR-TEM, which are marginally higher than the targeted value of 2.4 nm (Figure 10). This may be an artefact of the broadened size distributions for continuously synthesized nanoparticles with standard deviations of ±0.45, ±0.48, and ±0.40 nm for the different combinations A, B, and C, respectively (±0.23nm for batch procedure). Since there is little difference in the particle sizes of the Pt nanoparticles produced via the different syringe combinations, combination C is selected due to the narrow particle size distribution in combination with the largest volume of nanoparticle suspension facilitating the scale-up of the synthesis procedure. The synthesis volume is twice as high as in the standardized batch synthesis, while the continuous synthesis may be easily scaled further.

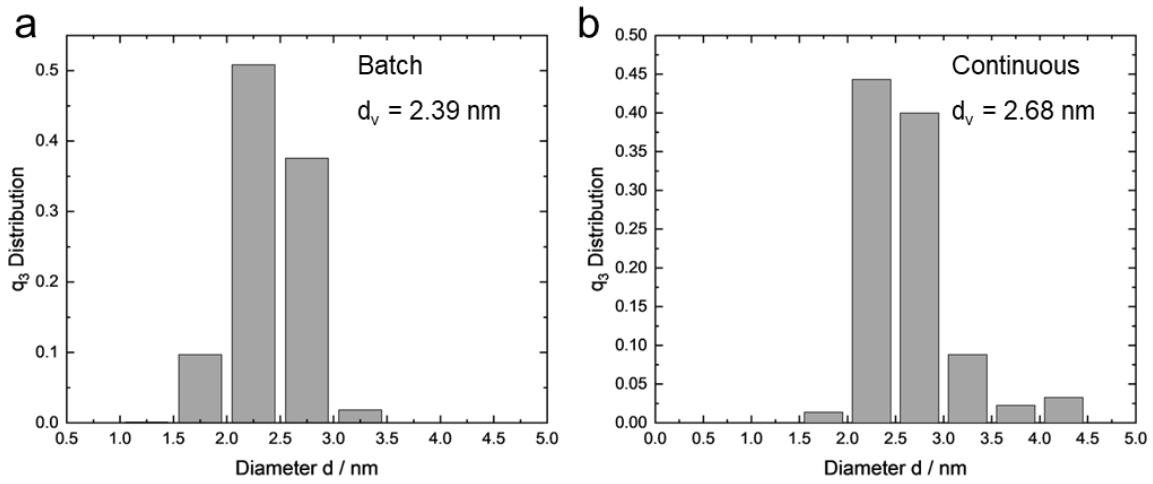

Figure 10: Pt nanoparticle size distributions for Pt/Al_2O_3 catalysts synthesized via (a) batch and (b) continuous procedure. Synthesis conditions: Batch procedure with PVP:Pt ratio = 5 g_{PVP} g_{Pt}^{-1}, $NaBH_4$:Pt ratio = 0.47 mol_{NaBH4} mol_{Pt}^{-1}, c_{NaOH} = 10 mM. Continuous procedure with syringe combination C, $F_{big\ syringe}$ = 0.84 mL·min^{-1}, PVP:Pt ratio = 5 g_{PVP} $_{Pt}^{-1}$, $NaBH_4$:Pt ratio = 0.47 mol_{NaBH4} mol_{Pt}^{-1}, c_{NaOH} = 10 mM.

In order to achieve a defined Pt nanoparticle size, the influence of the amount of reducing agent on the Pt particle size was also investigated for the continuous process. For this purpose, several stock solutions with different concentrations of the reducing agent $NaBH_4$ were prepared and subsequently used in the continuous colloidal synthesis with chemical reduction. The general correlation between the $NaBH_4$:Pt ratio and the Pt nanoparticle size in the continuous synthesis is comparable to the batch synthesis, but the obtained sizes are constantly 0.2 to 0.3 nm larger for the same $NaBH_4$:Pt ratio. Once again, a plateau at 2.8 nm was observed for high ratios (Figure 11).

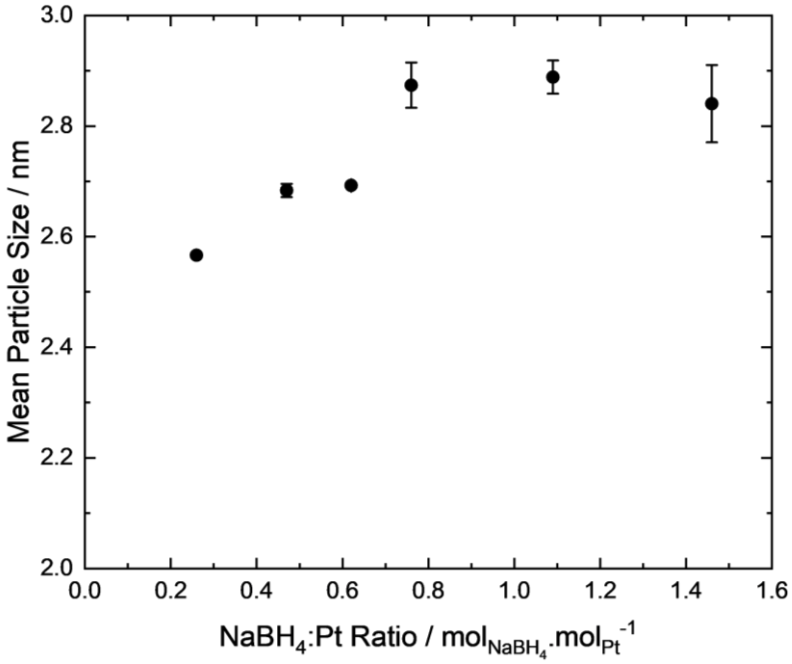

Figure 11: Influence of the specific amount of basic reducing agent $NaBH_4$ on the size of Pt nanoparticles from the continuous colloidal synthesis process with chemical reduction. Synthesis conditions: Continuous procedure with syringe combination C (100 mL, 30 mL), $F_{big\ syringe} = 0.84$ mL min^{-1}, PVP:Pt ratio = 5 g_{PVP} g_{Pt}^{-1}. Error bars represent standard deviation for three reproductions.

Furthermore, the performance of the continuously synthesized Pt/Al_2O_3 catalysts in the dehydrogenation of H12-BT was evaluated at a reaction temperature of 230 °C to amplify potential differences in the performance (Figure 12). A catalyst with the same particle size from the batch synthesis procedure is used as benchmark. Both catalysts show a similar performance indicating that the continuous synthesis route may be applied for the production of dehydrogenation catalysts and, apart from the slightly increased particle size, has no influence on the activity of the obtained catalysts.

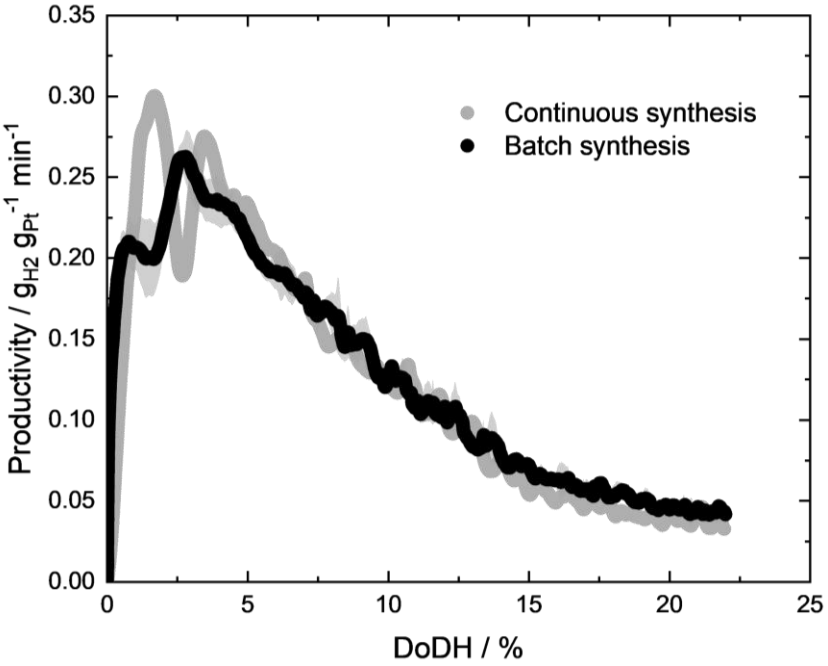

Figure 12: Productivity as a function of degree of dehydrogenation (DoDH) during semi-batch dehydrogenation of H12-BT using Pt/Al_2O_3 powder catalysts with platinum particle sizes of 2.4 nm, synthesized via batch and continuous synthesis routes. Reaction conditions: T = 230 °C, $n_{Pt}:n_{LOHC}$ = 0.1 mol.%, F_{Ar} = 300 mL·min^{-1}, $t_{Reaction}$ = 120 min, catalyst loading = 0.2 wt.% Pt. Synthesis conditions: Batch (black) and continuous (grey) procedure with powders, PVP:Pt ratio = 5 g_{PVP} g_{Pt}^{-1}, $NaBH_4$:Pt ratio = 0.31 mol_{NaBH4} mol_{Pt}^{-1}, C_{NaOH} = 10 mM.

Summary

In this work, a colloidal approach in combination with chemical reduction was optimized for the synthesis of well-defined Pt nanoparticles. After immobilization on Al_2O_3 support materials, the supported catalysts were employed in the dehydrogenation of the LOHC H12-BT without further pre-treatment. Different parameters were varied during the synthesis to evaluate their influence on the size of the Pt nanoparticles. The amount of the steric stabilizer PVP showed only a marginal effect on the platinum particle size for the studied range of PVP:Pt ratios. To minimize its potential effect on catalysis, the lowest ratio of 5 g_{PVP} g_{Pt}^{-1} was used. Similarly, the influence of the reducing agent $NaBH_4$ on Pt nanoparticle size was investigated. Supported nanoparticles in the size range of 2.0 to 6.0 nm were synthesized, while the amount of reducing agent scales with the nanoparticle size in agreement with theoretical models of particle formation. The use of basic $NaBH_4$ solutions allows for a more precise control of the Pt nanoparticle size up to 2.8 nm, while increasing the temporal stability of the reduction solution enabling its use in continuous synthesis. To provide well-defined catalyst samples for studies in technical LOHC dehydrogenation reactors, the

immobilization of the prepared Pt nanoparticles was transferred from powder to shaped supports by using hollow Al_2O_3 cylinders. Despite possible limitations due to mass transport effects, the shaped catalysts showed only minor differences in catalytic performance compared to powder catalysts. Finally, the continuous synthesis of Pt nanoparticles using a microfluidic reactor was demonstrated. Analogous to the observations from batch syntheses, the size of the Pt nanoparticles in the continuous syntheses was also mainly linked to the amount of reducing agent. Catalysts synthesized via the continuous procedure showed similar catalytic performance in the dehydrogenation of H12-BT as a comparable catalyst from batch synthesis.

Acknowledgments

Financial support by the Bavarian Ministry of Economic Affairs, Regional Development and Energy through the project "Emissionsfreier und stark emissionsreduzierter Bahnverkehr auf nicht-elektrifizierten Strecken" and by the Helmholtz Research Program "Materials and Technologies for the Energy Transition (MTET), Topic 3: Chemical Energy Carriers" is highly acknowledged. Infrastructural support by DFG via its SFB 1452 (Catalysis at Liquid Interfaces, CLINT) is also gratefully acknowledged.

Conflicts of interest

Peter Wasserscheid is the co-founder and minority shareholder of Hydrogenious LOHC Technologies GmbH, Erlangen, a company that has commercialised equipment for hydrogen storage using the LOHC technology.

References

[1] A. Le Valant, C. Comminges, F. Can, K. Thomas, M. Houalla, F. Epron, *The Journal of Physical Chemistry C* **2016**, *120*, 26374-26385.
[2] F. Auer, A. Hupfer, A. Bösmann, N. Szesni, P. Wasserscheidpeter, *Catalysis Science & Technology* **2020**, *10*, 6669-6678.
[3] G. A. Somorjai, J. Carrazza, *Industrial & Engineering Chemistry Fundamentals* **1986**, *25*, 63-69.
[4] H. Lee, S. E. Habas, S. Kweskin, D. Butcher, G. A. Somorjai, P. Yang, *Angewandte Chemie International Edition* **2006**, *45*, 7824-7828.

[5] G. A. Somorjai, Y. Li, *Introduction to surface chemistry and catalysis*, Wiley, Hoboken (New Jersey), **2010**.
[6] K. G. Papanikolaou, M. Stamatakis, *Catalysis Science & Technology* **2020**, *10*, 5815-5828.
[7] R. K. Herz, W. D. Gillespie, E. E. Petersen, G. A. Somorjai, *Journal of Catalysis* **1981**, *67*, 371-386.
[8] S. M. Davis, G. A. Somorjai, *Journal of Catalysis* **1980**, *65*, 78-83.
[9] G. A. Somorjai, D. W. Blakely, *Nature* **1975**, *258*, 580-583.
[10] B. A. T. Mehrabadi, S. Eskandari, U. Khan, R. D. White, J. R. Regalbuto, **2017**, pp. 1-35.
[11] C. Perego, P. Villa, *Catalysis Today* **1997**, *34*, 281-305.
[12] D. Strauch, P. Weiner, B. B. Sarma, A. Körner, E. Herzinger, P. Wolf, A. Zimina, A. Hutzler, D. E. Doronkin, J.-D. Grunwaldt, P. Wasserscheid, M. Wolf, *Catalysis Science & Technology* **2024**, *14*, 1775-1790.
[13] S. Kaneko, M. Izuka, A. Takahashi, M. Ohshima, H. Kurokawa, H. Miura, *Applied Catalysis A: General* **2012**, *427-428*, 85-91.
[14] O. S. Alexeev, S. Y. Chin, M. H. Engelhard, L. Ortiz-Soto, M. D. Amiridis, *The Journal of Physical Chemistry B* **2005**, *109*, 23430-23443.
[15] A. Goguet, D. Schweich, J. P. Candy, *Journal of Catalysis* **2003**, *220*, 280-290.
[16] J. T. Miller, M. Schreier, A. J. Kropf, J. R. Regalbuto, *Journal of Catalysis* **2004**, *225*, 203-212.
[17] M. K. Oudenhuijzen, P. J. Kooyman, B. Tappel, J. A. van Bokhoven, D. C. Koningsberger, *Journal of Catalysis* **2002**, *205*, 135-146.
[18] D. Zakgeym, T. Engl, Y. Mahayni, K. Müller, M. Wolf, P. Wasserscheid, *Applied Catalysis A: General* **2022**, *639*, 118644.
[19] J. T. Miller, M. Schreier, A. J. Kropf, J. R. Regalbuto, *Journal of Catalysis* **2004**, *225*, 203-212.
[20] J. A. Moulijn, A. E. van Diepen, F. Kapteijn, *Applied Catalysis A: General* **2001**, *212*, 3-16.
[21] H. Nagao, M. Ichiji, I. Hirasawa, *Chemical Engineering & Technology* **2017**, *40*, 1242-1246.
[22] S. C. Jung, S. W. Nahm, H. Y. Jung, Y. K. Park, S. G. Seo, S. C. Kim, *Journal of Nanoscience and Nanotechnology* **2015**, *15*, 5461-5465.
[23] S. A. Gama-Lara, R. A. Morales-Luckie, L. Argueta-Figueroa, J. P. Hinestroza, I. García-Orozco, R. Natividad, *Journal of Nanomaterials* **2018**, *2018*, 1-8.
[24] D. Pham Minh, Y. Oudart, B. Baubet, C. Verdon, C. Thomazeau, *Oil & Gas Science and Technology - Revue de l'IFP* **2009**, *64*, 697-706.
[25] S. Kidambi, J. Dai, J. Li, M. L. Bruening, *Journal of the American Chemical Society* **2004**, *126*, 2658-2659.
[26] M. Liu, W. Yu, H. Liu, *Journal of Molecular Catalysis A: Chemical* **1999**, *138*, 295-303.
[27] K. Mavani, M. Shah, *International Journal of Engineering Research & Technology* **2013**, *3*, IJERTV2IS3605.
[28] H. Hiramatsu, F. E. Osterloh, *Chemistry of Materials* **2004**, *16*, 2509-2511.
[29] I. Hussain, S. Graham, Z. Wang, B. Tan, D. C. Sherrington, S. P. Rannard, A. I. Cooper, M. Brust, **2005**, *127*, 16398-16399.
[30] X. Zeng, B. Zhou, Y. Gao, C. Wang, S. Li, C. Y. Yeung, W. Wen, *Nanotechnology* **2014**, *25*, 495601.
[31] B. A. Mehrabadi, S. Eskandari, U. Khan, R. D. White, J. R. Regalbuto, *Advances in Catalysis* **2017**, *61*, 1-35.

[32] M. Willer, P. Preuster, M. Geißelbrecht, P. Wasserscheid, *International Journal of Hydrogen Energy* **2024**, *57*, 1513-1523.
[33] J. Kadar, F. Gackstatter, F. Ortner, L. Wagner, M. Willer, P. Preuster, P. Wasserscheid, M. Geißelbrecht, *International Journal of Hydrogen Energy* **2024**, *59*, 1376-1387.
[34] F. Auer, Dissertation thesis, Katalysatorentwicklung für die Dehydrierung von Perhydro-Dibenzyltoluol, Friedrich-Alexander-University (Erlangen), **2020**. https://open.fau.de/handle/openfau/14054
[35] A. M. Seidel, Dissertation thesis, Entwicklung eines technischen Platin-Trägerkatalysators zur Dehydrierung von Perhydro-Dibenzyltoluol, Friedrich-Alexander University (Erlangen) (Germany), **2019**. https://open.fau.de/handle/openfau/12386
[36] M. Geißelbrecht, S. Mrusek, K. Müller, P. Preuster, A. Bösmann, P. Wasserscheid, *Energy & Environmental Science* **2020**, *13*, 3119-3128.
[37] T. Rüde, S. Dürr, P. Preuster, M. Wolf, P. Wasserscheid, *Sustainable Energy & Fuels* **2022**, *6*, 1541-1553.
[38] T. Teranishi, M. Hosoe, T. Tanaka, M. Miyake, *The Journal of Physical Chemistry B* **1999**, *103*, 3818-3827.
[39] J. Yamamoto, *Rohm, H., Ed* **2003**.
[40] R. Retnamma, C. Rangel, A. Q. Novais, M. A. Matthews, *Symposium on Hydrogen, Fuel Cells and Advanced Batteries*, **2013**.
[41] J. Polte, X. Tuaev, M. Wuithschick, A. Fischer, A. F. Thuenemann, K. Rademann, R. Kraehnert, F. Emmerling, *ACS Nano* **2012**, *6*, 5791-5802.
[42] J. Schindelin, C. T. Rueden, M. C. Hiner, K. W. Eliceiri, *Molecular Reproduction & Development* **2015**, *82*, 518-529.
[43] Sasol. GmbH, Produktkatalog Puralox Catalox
[44] J. E. Newton, J. A. Preece, N. V. Rees, S. L. Horswell, *Physical Chemistry Chemical Physics* **2014**, *16*, 11435-11446.
[45] W. Huang, Q. Hua, T. Cao, *Catalysis Letters* **2014**, *144*, 1355+.
[46] M. Wolf, N. Fischer, M. Claeys, *Materials Chemistry and Physics* **2018**, *213*, 305-312.
[47] N. T. Thanh, N. Maclean, S. Mahiddine, *Chemical Reviews* **2014**, *114*, 7610-7630.
[48] J. Bedia, J. Lemus, L. Calvo, J. J. Rodriguez, M. A. Gilarranz, *Colloids and Surfaces A: Physicochemical and Engineering Aspects* **2017**, *525*, 77-84.
[49] V. K. LaMer, R. H. Dinegar, *Journal of the American Chemical Society* **1950**, *72*, 4847-4854.
[50] J. M. M. Tengco, Dissertation thesis, Synthesis of Well Dispersed Supported Metal Catalysts by Strong Electrostatic Adsorption and Electroless Deposition, University of South Carolina, **2016**, https://www.proquest.com/openview/f6672a56d4004b6e43e19837ce11ebd5.
[51] W. Peters, A. Seidel, S. Herzog, A. Bösmann, W. Schwieger, P. Wasserscheid, *Energy & Environmental Science* **2015**, *8*, 3013-3021.
[52] R. E. Davis, C. G. Swain, *Journal of the American Chemical Society* **1960**, *82*, 5949-5950.
[53] P. R. Van Rheenen, M. J. McKelvy, W. S. Glaunsinger, *Journal of Solid State Chemistry* **1987**, *67*, 151-169.
[54] V. S. K. K. N. Mochalov, G. G. Gil'manshin, *Dokl. Akad. Nauk SSSR* **1965**, *162*, 613-616.
[55] S. Nishimura, A. Takagaki, S. Maenosono, K. Ebitani, *Langmuir* **2010**, *26*, 4473-4479.
[56] S. Marre, K. F. Jensen, *Chemical Society Reviews* **2010**, *39*, 1183-1202.
[57] G. Tofighi, H. Lichtenberg, J. Pesek, T. L. Sheppard, W. Wang, L. Schöttner, G. Rinke, R. Dittmeyer, J.-D. Grunwaldt, *Reaction Chemistry & Engineering* **2017**, *2*, 876-884.

[58] G. Tofighi, H. Lichtenberg, A. Gaur, W. Wang, S. Wild, K. Herrera Delgado, S. Pitter, R. Dittmeyer, J.-D. Grunwaldt, D. E. Doronkin, *Reaction Chemistry & Engineering* **2022**, *7*, 730-740.
[59] P. L. Suryawanshi, S. P. Gumfekar, P. R. Kumar, B. B. Kale, S. H. Sonawane, *Colloid and Interface Science Communications* **2016**, *13*, 6-9.